P12R.6

NCAR S-POL SECOND FREQUENCY (K_A-BAND) RADAR

Gordon Farquharson,* Frank Pratte, Milan Pipersky, Don Ferraro, Alan Phinney,
Eric Loew, Robert Rilling, Scott Ellis, and Jothiram Vivekanandan
National Center for Atmospheric Research, Boulder, Colorado

1. INTRODUCTION

The National Center for Atmospheric Research (NCAR) has recently extended the observational capability of the S-band dual-polarimetric weather radar system (S-Pol, Keeler et al. (2000)) by adding a K_a-band (35 GHz) polarimetric Doppler radar (Vivekanandan et al., 2004). The K_a-band radar employs a dual channel receiver and can be configured for either HH and HV, or HH and VV polarimetric measurements. The K_a-band and S-band antenna beams are matched and aligned, and timing signals for both systems are generated from the Global Position System (GPS) ensuring that a common resolution volume is sampled by both systems. This dual-wavelength capability provides the potential for retrieving water vapor profiles (Ellis et al., 2005) and liquid water content in Rayleigh scattering conditions (Vivekanandan et al., 1999), improving remote sensing of various precipitation types, and studies on cloud microphysics.

2. RADAR DESCRIPTION

The K_a-band radar is housed in three enclosures which are mounted to the S-Pol S-band dish and pedestal structure (Figure 1); these include the transmitter enclosure, the receiver enclosure, and the radar processor enclosure. The system does not rely on the S-Pol pedestal infrastructure, and requires only an AC power feed. This allows the K_a-band radar to be run independently from S-Pol for development and testing. The system is weather proof, and has been operated successfully during heavy rain.

Figure 2 shows an block diagram the K_a-band system. Dashed lines in the figure represent each of the enclosures. In the configuration shown, the transmitted power is split, and both H and V polarizations are transmitted simultaneously. The power divider in the transmit path can be replaced by waveguide that directs all of the transmitted power to one of the antenna ports thereby reconfiguring the radar to transmit a single polarization and receive on both.

The transmitter was built by Applied Systems Engineering and uses a Litton L-4046A magnetron which is specified to produce a 125 kW peak power pulse with a pulse length up to 1 μs. The transmitter enclosure is mounted to the S-Pol antenna counter weight (Figure 1). A combination of WG-28 and low loss Tallguide (TG-40) from Antennas for Communications is used to connect the transmitter enclosure to the receiver enclosure on which the K_a-band antenna is mounted. The

*Corresponding author address: Gordon Farquharson, NCAR/EOL, 1850 Table Mesa Dr., Boulder, CO 80303; e-mail: gordonf@ucar.edu

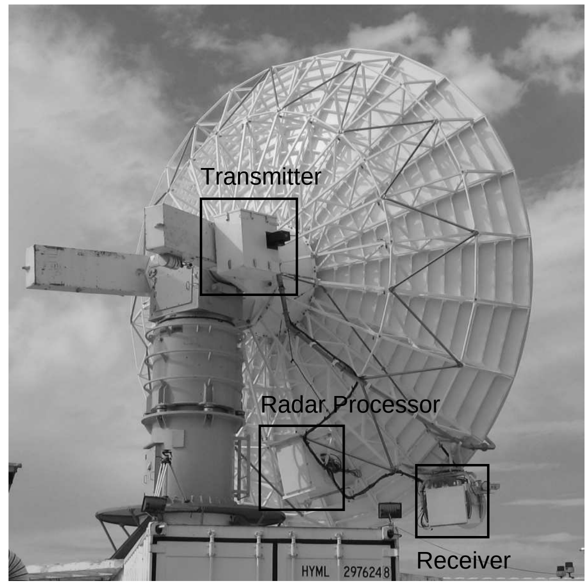

Figure 1: K_a-band radar attached to the S-band dish. The transmitter, receiver, and processor enclosures are visible. The K_a-band antenna is mounted to the receiver enclosure and is facing away from the viewer in the photograph.

Tallguide loss is around 3 dB/100 ft compared to around 17.5 dB/100 ft for WG-28, and the loss through the waveguide assembly is around 3.5 dB.

The receiver enclosure is mounted on the side of the S-band dish. It contains a dual-channel receiver front-end (H and V polarizations), electronics to down-convert received signals to an intermediate frequency (IF, 132.5 MHz), and the K_a-band antenna. The receiver uses a super heterodyne structure to keep the receiver center frequency tuned to the magnetron frequency. The first local oscillator is tunable from 32 to 35 GHz, but is usually set to a fixed frequency for a particular magnetron. This down-converts the received signal to a range between 1532 to 1932 MHz. The second local oscillator is tunable from 1400 to 1800 MHz, and is constantly changed such that the IF signal is centered within 1 MHz of 132 MHz. The last down-conversion stage is implemented on the digitizing cards in the radar processor, and down-converts the IF to 25 MHz and samples the result. This local oscillator is tunable from 95 to 120 MHz in 100 kHz steps. Thus the center frequency of the sampled signal is always within 100 kHz of the receiver center frequency.

The IF signals are sent to the processor which is housed directly behind the S-band dish. The radar pro-

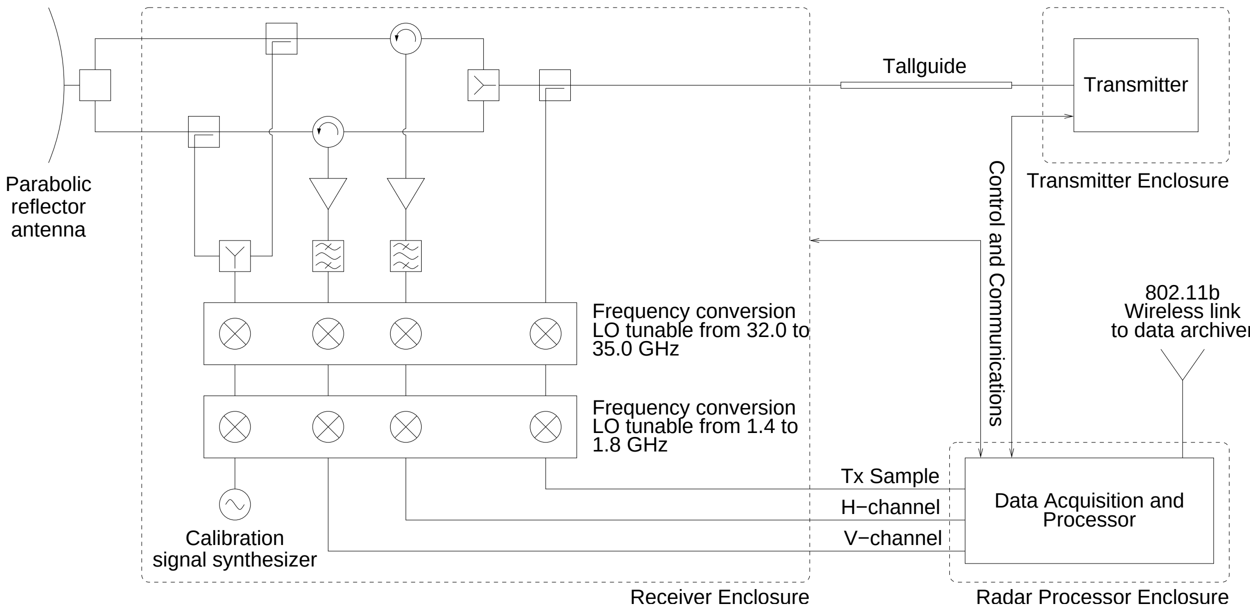

Figure 2: K_a-band block diagram. Dashed lines represent the three enclosures housing the K_a-band radar. The antenna is mounted to the receiver enclosure.

cessor uses Binet Sampler cards originally designed for a bistatic network of radars. Timing signals generated by these cards are synchronized with GPS to ensure that the resolution of the K_a-band radar volumes are matched with the S-band resolution volumes. These cards band limit the 25 MHz IF signals and sample the waveform at a 20 MHz sampling rate. Digital IF filtering and demodulation is performed in hardware. The radar processor computes moments from the raw data and transmits these to the S-Pol data archiver over an 802.11b wireless link. This connection is also used to access the graphical user interface for control and real-time display.

A separate channel in the receiver is used to sample the transmitted pulse. These samples are used to determine the phase and frequency of the transmitted pulse. The phase is used to adjust the phase of the received echos to a common phase reference such that Doppler velocity and differential phase can be computed. The frequency is used to tune the local oscillator frequencies to adjust the receiver center frequency for changes in the magnetron frequency. The receiver also contains a calibration signal which is injected into the front-end of both channels to track differential gain changes. This signal occupies three range gates near the end of the range swath recorded by the radar.

The K_a-band antenna is built by Seavey Engineering. The antenna consists of a 28 inch solid parabolic reflector with a 9 inch focal length, and a dual polarized feed assembly. Both co- and cross-polarization sidelobes are below -26 dB, and the polarization isolation was measured at below 31 dB. An important requirement for dual-wavelength measurements is that both radars sample the same resolution volume at the same time. The S- and K_a-band radar beams are aligned using solar scans, and both radars derive system timing from GPS to ensure that the resolution volumes are illuminated at the same time and samples are recorded simultaneously.

Table 1: K_a-band Radar Operating Parameters

Transmit Frequency	34.7–35.0 GHz
Peak Transmit Power	15 kW
Pulse Repetition Frequency	500 Hz
Pulse Length	0.8 μs
Antenna	Parabolic Reflector
Antenna Diameter	0.7 m
Antenna Gain	45 dB
Antenna Beamwidth	0.93 degrees
Minimum Detectable Signal @ 10 km	-25 dBZ

Table 1 lists nominal system parameters for the K_a-band system. These numbers are based on the single polarization transmit configuration for the radar.

3. POLARIMETRIC CAPABILITIES

The K_a-band system can be reconfigured for either transmit H and receive both H and V polarizations (HH/HV), or simultaneous transmit and receive both H and V polarizations (HH/VV) modes. Polarimetric variables available using the HH/HV scheme are L_{DR}, and using the HH/VV scheme are Z_{DR}, $|\rho_{hv}|$, and ϕ_{DP}.

4. EXAMPLE DATA

The system was fielded three times in 2004: Winter Icing Storms Project 2004 (WISP), North American Monsoon Experiment (NAME), and Rain in Cumulus over the Ocean (RICO). Figure 3 shows radar images of reflectivity and Doppler velocity from the S- and K_a-band radars collected during the RICO project. The S-band Doppler image (Figure 3(b)) shows that the wind is from the east. Both the S-and K_a-band radar reflectivity images (Figures 3a,b) show scattering from clouds and rain in the upper half of the plots. In this region, S-band reflectivity values range from 5 to 35 dBZ, and K_a-band reflectivity values range from -10 to 20 dBZ. In most other regions, Bragg scattering is evident in the S-band image, but the K_a-band sees virtually no reflections. Because of this, Most of the K_a-band velocity image (Figure 3d) is noisy, but in regions of good signal to noise ratio, the K_a-band Doppler velocity is folded. It should be noted that K_a-band velocities include a component from the movement of the K_a-band dish since the dish is not located at the center of rotation.

5. FUTURE UPGRADES

During RICO, various problems were identified with the K_a-band system. The Litton L-4064A magnetron has a typical lifetime of only 200 hours. This is not suitable for extended field programs that require operation 24 hours a day. An alternate magnetron, the SFD-319, has been selected. Typical lifetimes for this magnetron are in excess of 10,000 hours. The peak power output is 120 kW which is 5 kW (0.2 dB) less than the L-4064A, but is only capable of producing a pulse length of 0.5 μs. However, the loss in sensitivity due to the shorter pulse length can be mostly compensated for by doubling the pulse repetition frequency of the system. This magnetron will allow for reliable deployment of the K_a-band system for extended periods without maintenance and the necessary recalibration of the system associated with different magnetrons.

Mechanical stresses on front-end cables in the receiver were also found after RICO. Receiver upgrades are currently being implemented. The front-end electronics will be remounted onto a thermally stable metal plate, and connected with rigid coaxial cable. This should improve the stability of the receiver channels, and prevent wear on the K_a-band cables as the structure moves. Furthermore, the transmit and calibration signal power will be independently monitored to track changes. This will improve determination of calibration constants used in post-processing.

A problem with the calibration signal was also identified during the RICO deployment. The cause of this problem was isolated to the calibration signal up-conversion electronics, and this has been redesigned.

Finally, errors were found the radar data acquisition system and processor. There was a fractional range gate shift between the receiver channel samples, which caused large Z_{DR} values in regions of large gradients in reflectivity. In addition, ghost echos of existing features, displaced in azimuth, appear in the data. The problem has been narrowed down to code in the radar processor, and will be fixed before the next deployment of the K_a-band system.

6. SUMMARY

The addition of a K_a-band radar strengthens S-Pol as a unique remote sensing tool available to the atmospheric research community by allowing researchers to conduct dual-wavelength studies. The system is readily transportable, and comprises a small fraction of the operating cost to field programs involving S-Pol. The system has already participated in three field projects, and current upgrades will further improve the quality of the data produced by the radar.

7. ACKNOWLEDGEMENT

Portions of this work were sponsored by the National Science Foundation through an inter-agency agreement in response to requirements and funding from the Federal Aviation Administration's Aviation Weather Research Program. The view expressed in the paper are those of the authors and do not necessarily represent the official policy position of the U.S. government.

REFERENCES

Ellis, S., K. Goodman, J. Vivekanandan, and C. Kessinger, 2005: Water vapor and liquid water estimates using simultaneous s and ka band radar measurements. *32nd Conf. on Radar Meteor.*, AMS.

Keeler, R. J., J. Lutz, and J. Vivekanandan, 2000: S-Pol: NCAR's polarimetric Doppler research radar. *Proceedings of the International Geoscience and Remote Sensing Symposium*, IEEE, Honolulu, Hawaii, 1570–1573.

Vivekanandan, J., B. E. Martner, M. K. Politovich, and G. F. Zhang, 1999: Retrieval of atmospheric liquid and ice characteristics using dual-wavelength radar observations. *IEEE Trans. Geosci. Remote Sens.*, **37**, 2325–2334.

Vivekanandan, J., M. Politovich, R. Rilling, S. Ellis, and F. Pratte, 2004: Sensitivity of S- and Ka-band matched dual-wavelength radar system for detecting non-precipitating cloud. *Microwave Remote Sensing of the Atmosphere and Environment IV*, G. Skofronick Jackson and S. Uratsuka, eds., SPIE, Honolulu, Hawaii, volume 5654 of *Proceedings of the SPIE*, 14–24.

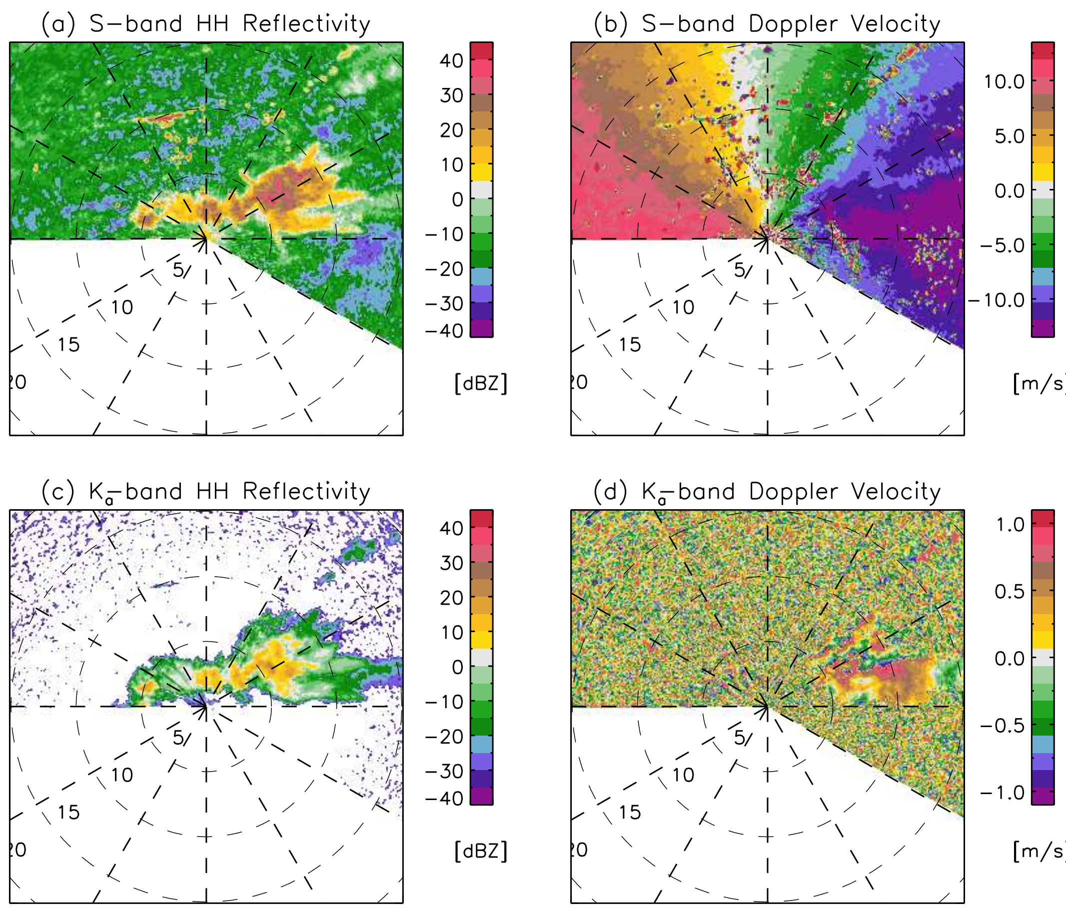

Figure 3: S- and K_a-band radar data collected during the RICO project at 14:48 on January 1, 2005. The elevation angle is 1.5 degrees. Concentric dashed rings indicate radial distance from the radar.